

Interactive Model for Energy Management of Clustered Microgrids

Tianguang Lu, *Sudent Member, IEEE*, Zhaoyu Wang, *Member, IEEE*, Qian Ai, *Member, IEEE*, and Wei-Jen Lee, *Fellow, IEEE*

Abstract—The increasing integration of distributed renewable energy resources highlights the need to design new control strategies for hybrid WT-PV-battery microgrid clusters. This paper proposes a two-level optimization model for the coordinated energy management between distribution systems and clustered WT-PV-battery microgrids (MGs). The upper level of the model deals with the operation of the distribution network, while the lower level considers the coordinated operation of multiple MGs. An interactive game matrix (IGM) is applied to coordinate the power exchange among multiple MGs and between the distribution network and MGs. The model is solved by a modified hierarchical genetic algorithm. Case studies on a distribution system with MGs as well as a practical multi-MG system demonstrate the effectiveness of the proposed method in improving power quality, reliability, and environmental benefits.

Index Terms—power distribution systems; renewable energy integration; microgrids; energy management; responsive reserve

NOMENCLATURE

Sets

I	set of distribution network nodes
I^g	set of distribution network nodes with micro turbines (MTs) and static VAR compensations (SVGs)
I^M	set of distribution network nodes with MGs
T	set of operation periods
F_N	set of MGs requesting power or power storage support
F	set of MGs
S_f	set of DGs and storage battery (SB), $f=1, 2, 3$, and 4 denote MT, SB, photovoltaic generator (PV) and wind turbine (WT), respectively
H_f	set of MGs supporting MG $_f$
S^D	set of MG $_i$ requesting power support in S
S^P	set of MG $_j$ providing power support in S

Variables

$R_{f,t}^{\text{EX}}$	variable of interactive game matrix (IGM)
$C_{f,t}$	cost of $R_{f,t}^{\text{EX}}$
$V_{i,t}$	voltage
P_t^{LS}	power loss of distribution network
$P_{i,t}^{\text{PED}} / Q_{i,t}^{\text{PED}}$	active/reactive power exchange between MG and distribution network at upper level
$P_{f,t}^{\text{PE}} / Q_{f,t}^{\text{PE}}$	active/reactive power exchange between MG $_f$ and distribution network at lower level

Manuscript received July 29, 2016; revised November 8, 2016; accepted January 2, 2017, 2015. This work was supported in part by National Natural Science Foundation of China (No. 51577115), and Iowa Energy Center.

T. Lu and Q. Ai are with the Department of Electrical Engineering, Shanghai Jiao Tong University, Shanghai 200240 China (e-mail: ltghao@163.com; aiqian@sjtu.edu.cn)

Z. Wang is with the Department of Electrical and Computer Engineering, Ames, IA 50011 USA (e-mail: wzy@iastate.edu)

W. Lee is with the Energy Systems Research Center, University of Texas at Arlington, TX 76019 USA (e-mail: wlee@uta.edu)

$P_{i,t}^g / Q_{i,t}^g$	active/reactive power of MT and static VAR compensation (SVC)
$\theta_{i,j,t}$	phase angle difference between i and j
g_1 / g_2	dispatchable capacity of MT/SB in MGs
k_i	binary variable of g_i
k_n^1	binary variable of g_n^1
k_m^2	binary variable of g_m^2
$P_{s,f,t}^G / Q_{s,f,t}^G$	active/reactive power of DG $_s$ and SB in MG $_f$
$x_{h,t} / y_{h,t}$	binary variable of $P_{h,t}^{\text{MTEX}} / P_{h,t}^{\text{SBEX}}$ to determine whether it is carried out
$P_{h,t}^{\text{MTEX}} / P_{h,t}^{\text{SBEX}}$	remaining dispatchable capacity of MT/SB in MG $_h$ supporting MG $_f$
$a_{f,t} / b_{f,t}$	binary variables of $P_{f,t}^{\text{MTEX}} / P_{f,t}^{\text{SBEX}}$ to determine whether it is carried out
$E_{f,t}^{\text{T}}$	transition state of charge (SOC) of SB in MG $_f$
$E_{f,t}$	SOC of SB in MG $_f$
$\alpha_{h,t} / \beta_{h,t}$	maximum permissible remaining dispatchable capacity in $P_{h,t}^{\text{MTEX}} / P_{h,t}^{\text{SBEX}}$

<i>Parameters</i>	
$P_{i,t}^{\text{L}} / Q_{i,t}^{\text{L}}$	active/reactive load of node $_i$
η	power exchange degree
$G_{i,j} / B_{i,j}$	conductance/susceptance of line $i-j$
$P^{\text{PEmax}} / P^{\text{PEmin}}$	maximum/minimum power exchange
$P_i^{\text{max}} / P_i^{\text{min}}$	maximum/minimum output of MT and SVC in upper level
$Q^{\text{PEmax}} / Q^{\text{PEmin}}$	maximum/minimum reactive power exchange
$Q_i^{\text{max}} / Q_i^{\text{min}}$	maximum/minimum reactive output of MT and SVC in upper level
$P_h^{\text{MTmax}} / P_h^{\text{MTmin}}$	maximum/minimum output of MT in MG $_h$
$Q_h^{\text{MTmax}} / Q_h^{\text{MTmin}}$	maximum/minimum reactive output of MT in MG $_h$
$P_h^{\text{SBmax}} / P_h^{\text{SBmin}}$	maximum/minimum output of SB in MG $_h$
$Q_h^{\text{SBmax}} / Q_h^{\text{SBmin}}$	maximum/minimum reactive output of SB in MG $_h$
$V_i^{\text{max}} / V_i^{\text{min}}$	maximum/minimum voltage at node $_i$
q	sale/purchase price of grid
K_s^{FUEL}	fuel cost
K_s^{OM}	operation & maintenance cost
$P_{f,t}^{\text{ML}} / Q_{f,t}^{\text{ML}}$	active/reactive load in MG $_f$
R_t	original responsive reserve of distribution network
R_t^{MC}	responsive reserve of MG cluster
R_t^{OMC}	original spare capacity of MG cluster
$E_f^{\text{max}} / E_f^{\text{min}}$	maximum/minimum capacity of SB in MG $_f$
$R^{\text{up}} / R^{\text{down}}$	ramp up/down coefficient of MT
p_x	emission penalty
$N_{x,s}$	DG emissions
α	limit parameter of $P_{h,t}^{\text{MTEX}}$
ε	coefficient of reserve support degree from MG cluster to distribution network

I. INTRODUCTION

The integration of distributed energy resources (DERs) is a promising solution to restructure the current distribution

network and increase the reliability of energy supply [1-3]. Microgrids (MGs) are smart clusters of distributed generators (DGs), loads and energy storage systems (ESS) [4-5]. MGs can facilitate the integration and operation of DERs [6-8]. Multiple microgrids can be connected to a modern distribution system to further improve the operation, reliability, economic benefits, and environmental friendliness [9-10]. However, the integration of clustered MGs poses new challenges on the system energy management [11].

The operation and control of a distribution system with MGs has been well studied in existing literature. The coordinated control in the distribution network including MGs can be considered as a tri-level hierarchical system with the primary droop control of power electronic inverters, the secondary control for *V/F* restoration and synchronization, and the tertiary control for *P/Q* import and export [12]. The third level, which is related to energy management, is the main subject of this paper [13]. An energy management unit based on a multi-agent system was presented in [14] to improve economic benefits and system operations of a stand-alone MG. Reference [15] introduced a modified concept of multi-carrier energy hub and integrated it with the modeling of a MG. The above mentioned work considered the energy management of a single MG. The authors in [16] proposed leader-follower strategies for the energy management of multiple MGs. The study in [17] developed a stochastic model to regulate the power exchange between a utility grid and the connected MGs. An intelligent energy and thermal comfort management was established in [18] for grid-connected microgrids with a heterogeneous occupancy schedule. These studies focused on the single-period dispatch without ESS. Reference [19] leveraged demand side management to reduce the peak demand and maximize customers' benefits in a smart distribution system with multiple MGs. Reference [20] introduced a statistical cooperative dispatch method to minimize the operation cost of a distribution system with multiple MGs. The authors in [21] proposed a stochastic game theory-based method for the coordinated energy management of networked MGs. All of the above-mentioned studies used economic benefits as the objective in performing the optimal energy management. In addition to economic benefits, to achieve improved system operations, such as flattened voltage profiles and increased reliability, is of great importance for a modern distribution system with clustered MGs.

This paper proposes a two-level energy management model for the interactive operation of a distribution network with clustered MGs [22]. An interactive game matrix (IGM) is developed to model the interactions among MGs. The IGM can take full advantage of remaining dispatchable capacity in ESS (i.e., storage battery (SB) in this paper) and DGs. The objectives of the upper level energy management are to minimize power exchange fluctuation, voltage deviation and power loss. The objectives of the lower level energy management are to minimize operation costs and the pollution emission. The lower level also offers responsive reserve support to the upper level. The two-level optimization problem is solved using a modified hierarchical genetic algorithm. Case studies are performed on an IEEE 14-bus test system with three MGs and a practical multi-MG system in China.

The main contributions of this paper can be summarized as follows:

- 1) A multi-period optimal dispatch model is proposed for a distribution network with clustered MGs.
- 2) Responsive reserve of DGs and remaining dispatchable capacity of ESS and controllable DGs are introduced to the model to improve the system operation.

3) Interactive game matrix (IGM) is defined to mathematically model coordinated operations of clustered MGs and the distribution network using game theories.

This paper is organized as follows. Section II presents the concept of clustered MG-based distribution systems. The two-level energy management model is presented in Section III. Section IV introduces the behavior analysis and interactive game matrix that is used for modelling the interactions among MGs. The solution algorithm is introduced in Section V. In Section VI, case studies on a distribution system with three MGs are provided. Section VII concludes the paper with major findings.

II. DISTRIBUTION SYSTEM WITH CLUSTERED MICROGRIDS

A. Distribution system with clustered MGs

Fig. 1 shows a distribution system with clustered MGs. The proposed model in this paper is integrated into a local energy management system (EMS). The EMS generates dispatch strategies based on the proposed model and the forecasting load/generation data. The objective of the proposed two-level model is to coordinate the energy management of the distribution grid and MGs to improve the system-wide efficiency.

In this paper, MGs are connected to different nodes in a distribution system. For example, if MG1 needs to send power to MG3, it should firstly exchange the power with the distribution grid and then MG3 receives the same amount of power minus the network losses from the distribution grid. Therefore, the distribution grid acts as a platform for the power exchange among MGs.

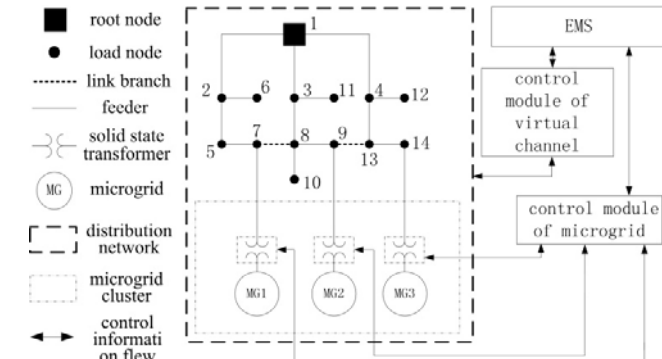


Fig. 1. The modified IEEE 14-bus distribution system with clustered MGs

B. Power reserve mechanism

In this paper, it is assumed that the available power reserve includes the responsive reserve and the remaining dispatchable capacity.

Some DGs such as Micro Turbines (MTs) and Wind Turbines (WTs) are spinning generators. Hence their reserve can be scheduled. In our model, these DGs in a MG cluster contribute to the system responsive reserve through the interaction between their hosting MGs and the distribution network to improve the system reliability.

The remaining dispatchable capacity comes from ESS and controllable DGs (e.g., MTs in this paper). For instance, if the SB in MG1 has stored energy, or the MT in MG1 does not reach its generation limit, the stored power or the remaining generation capacity can be sent to MG2 or MG3. Meanwhile, MG2 or MG3 can also store energy in the SB in MG1.

C. Two-level Coordinated Energy Management

The energy management model is formulated as a two-level optimization problem [23]. The upper level represents the interaction between clustered MGs and the distribution network.

The lower level models the interaction among MGs. Both levels have multiple objectives. Exchanging variables between the upper and lower levels are $P_{\text{PED},i,t}$, $Q_{\text{PED},i,t}$, $P_{\text{PE},i,t}$, $Q_{\text{PE},i,t}$ and the responsive reserve. Different MGs interact with each other by exchanging the remaining dispatchable capacity. The structure of the two-level model is shown in Fig. 2.

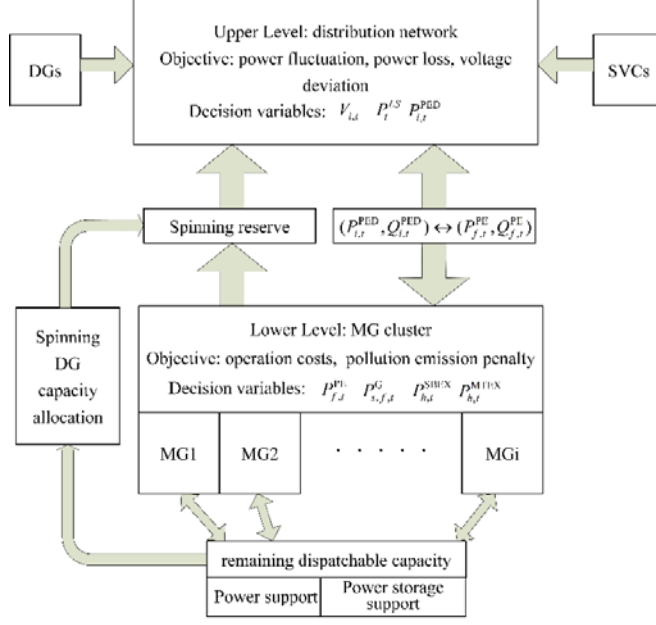


Fig. 2. Structure of the two-level model

III. OPTIMIZATION MODEL OF DISTRIBUTION SYSTEM

A. Mathematical formulation for upper level

The mathematical formulation of the upper-level model is described as follows:

$$\min F^{\text{up}} = \mu_1 F_1 + \mu_2 F_2 + \mu_3 F_3 \quad (1)$$

$$F_1 = \sum_{t=1}^T \sqrt{\sum_{i \in I} (V_{i,t} - 1)^2 / I} \quad (2)$$

$$F_2 = \sqrt{\sum_{t=1}^T \left(\sum_{i \in I^M} P_{i,t}^{\text{PED}} - \eta \right)^2 / T} \quad (3)$$

$$F_3 = \sum_{t=1}^T P_t^{\text{LS}} \quad (4)$$

s. t.

$$\begin{cases} P_{i,t}^g - P_{i,t}^L - P_{i,t}^{\text{PED}} = \\ V_{i,t} \sum V_{j,t} (G_{i,j} \cos \theta_{i,j,t} + B_{i,j} \sin \theta_{i,j,t}) \\ Q_{i,t}^g - Q_{i,t}^L - Q_{i,t}^{\text{PED}} = \\ V_{i,t} \sum V_{j,t} (G_{i,j} \sin \theta_{i,j,t} + B_{i,j} \cos \theta_{i,j,t}) \end{cases} \quad (5)$$

$$\begin{cases} P_{i,t}^g - P_{i,t-1}^g \leq R^{\text{up}} \\ P_{i,t-1}^g - P_{i,t}^g \leq R^{\text{down}} \end{cases} \quad (6)$$

$$\begin{cases} P_{i,t}^{\text{PE min}} \leq P_{i,t}^{\text{PED}} \leq P_{i,t}^{\text{PE max}} \\ P_i^{\text{g min}} \leq P_i^{\text{g}} \leq P_i^{\text{g max}} \\ Q_i^{\text{PE min}} \leq Q_i^{\text{PED}} \leq Q_i^{\text{PE max}} \\ Q_i^{\text{g min}} \leq Q_i^{\text{g}} \leq Q_i^{\text{g max}} \\ V_i^{\text{min}} \leq V_{i,t} \leq V_i^{\text{max}} \\ P_{\text{line min}} \leq P_{i,j,t} \leq P_{\text{line max}} \end{cases} \quad (7)$$

$$\sum_{i \in I^S} (P_{i,t}^{\text{g max}} - P_{i,t}^g) \geq R_t - R_t^{\text{MC}} \quad (8)$$

In the above formulation, F_1 represents the voltage deviations of all nodes. F_2 describes the level of total power exchange fluctuation between distribution network and MGs. It is important to reduce the power exchange fluctuation since it may affect the power quality of customers and lead to voltage/frequency deviations [24]. Moreover, this fluctuation may also affect the reliability and operation costs of distribution systems [25]. F_3 indicates the total power losses of the distribution network. Penalty factors of F_1 , F_2 , and F_3 are denoted as μ_1 , μ_2 , and μ_3 , respectively. Constraints on power flows, outputs, voltages, line capacity, and the spare capacity of the distribution network are shown in (5)-(8).

B. Mathematical formulation for lower level

When the power generation and demand are not balanced in a MG, it can import power from or export to other MGs through the distribution system. The allocation of the support from other MGs depends on their remaining dispatchable capacities. The lower-level model is formulated as follows:

$$\min f^{\text{down}} = f_1 + f_2 \quad (9)$$

$$f_1 = \sum_{f \in F} \sum_{t=1}^T \left\{ \sum_{s \in S_f} [q P_{s,f,t}^{\text{PE}} + (K_s^{\text{FUEL}} + K_s^{\text{OM}}) P_{s,f,t}^{\text{G}} + C_{f,t} R_{f,t}^{\text{EX}}] \right\} \quad (10)$$

$$f_2 = \sum_{t=1}^T \sum_{f \in F} \sum_{s \in S_f} (p_{\text{CO}_2} \cdot N_{\text{CO}_2,s} + p_{\text{NO}_x} \cdot N_{\text{NO}_x,s} + p_{\text{SO}_2} \cdot N_{\text{SO}_2,s}) \cdot P_{s,f,t}^{\text{G}} \quad (11)$$

s. t.

$$\begin{cases} P_{f,t}^{\text{ML}} - \sum_{s \in S_f} P_{s,f,t}^{\text{G}} - P_{f,t}^{\text{PE}} = 0 \\ Q_{f,t}^{\text{ML}} - \sum_{s \in S_f} Q_{s,f,t}^{\text{G}} - Q_{f,t}^{\text{PE}} = 0 \end{cases} \quad (12)$$

$$\begin{cases} E_{f,t}^{\text{T}} = E_{f,t-1}^{\text{T}} - P_{2,f,t}^{\text{G}} \\ E_{f,t} = E_{f,t}^{\text{T}} - y_{f,t} P_{f,t}^{\text{SBEX}} \\ E_f^{\text{min}} \leq E_{f,t} \leq E_f^{\text{max}} \end{cases} \quad (13)$$

$$\begin{cases} P_f^{\text{MTmin}} \leq P_{1,f,t}^{\text{G}} + x_{f,t} P_{f,t}^{\text{MTEX}} \leq P_f^{\text{MTmax}} \\ -P_f^{\text{SBmax}} \leq P_{2,f,t}^{\text{G}} + y_{f,t} P_{f,t}^{\text{SBEX}} \leq P_f^{\text{SBmax}} \\ Q_f^{\text{MTmin}} \leq Q_{1,f,t}^{\text{G}} \leq Q_f^{\text{MTmax}} \\ -Q_f^{\text{SBmax}} \leq Q_{2,f,t}^{\text{G}} \leq Q_f^{\text{SBmax}} \end{cases} \quad (14)$$

$$\begin{cases} P_{1,f,t}^{\text{G}} + x_{f,t} P_{f,t}^{\text{MTEX}} - P_{1,f,t-1}^{\text{G}} \leq R_t^{\text{up}} \\ P_{1,f,t-1}^{\text{G}} - (P_{1,f,t}^{\text{G}} + x_{f,t} P_{f,t}^{\text{MTEX}}) \leq R_t^{\text{down}} \end{cases} \quad (15)$$

$$\sum_{f \in F} (P_f^{\text{MTmax}} - P_{1,f,t}^{\text{G}}) + \sum_{f \in F} E_{f,t} \geq R_t^{\text{OMC}} \quad (16)$$

$$\sum_{f \in F} R_{f,t}^{\text{EX}} \leq \varepsilon R_t^{\text{OMC}} \quad (17)$$

$$R_t^{\text{MC}} = (1 - \varepsilon) R_t^{\text{OMC}} \quad (18)$$

where f_1 represents the total operation costs of clustered MGs. The cost of power exchange between the distribution system and clustered MGs can be calculated using the grid price q . The penalty of pollution emission is modeled in f_2 . Constraints on power balance, SB capacities, DG outputs, ramping rates, and interactive responsive reserves are shown in (12)-(18). In equations (17) and (18), ε represents the allocation of the original spare capacity of MGs between the distributed network and MGs. This paper assumes that every MG contains one SB and one MT.

IV. OPERATION OF CLUSTERED MICROGRIDS

A. Behavior analysis

In this section, the mechanism of interactive operation in clustered MGs is analyzed with the theory of cooperative game and priority.

In the cooperative game theory, different players (i.e., MGs in this paper) can form different coalitions (i.e., a MG cluster in this paper) in the player set based on the benefit allocation strategy to pursue the maximum benefit. Let S and N denote a coalition of MGs and the player set of clustered MGs, respectively. The allocation strategy is optimal when S and N satisfy condition (19). This means individuals in coalitions can obtain more benefits than independent counterparts [26]:

$$\begin{cases} \mathbf{x} = (x_1, \dots, x_i) \\ \sum_{i=1}^n x_i = v(N) \\ \sum_{i \in S} x_i \geq v(S), \forall S \in N \end{cases} \quad (19)$$

where x_i and $v(\cdot)$ represent benefit function and characteristic function, respectively [24]. In the cooperative game theory $(N, v), N = \{1, 2, \dots, n\}$, assign every player i ($i \in N$) a real parameter x_i and form $\mathbf{x} = (x_1, \dots, x_i)$, which satisfy $x_i \geq v(\{i\})$, $\dots \sum_{i=1}^n x_i = v(N)$, then \mathbf{x} is the allocation strategy of S , and x_i is benefit function. $v(S)$ is the maximum utility of gaming between S and $N - S = \{i \mid i \in N, i \notin S\}$.

In a coalition S , there are at least a demander i ($i \in S^D$) and a provider j ($j \in S^P$). We define $N_i = P_i^{\text{load}} - P_i$ as the power demand of i , where P_i^{load} means the load of MG $_i$, and P_i is generated by i to satisfy its load. Note the provider j only provides its remaining dispatchable capacity. Define λ as the utility parameter (\$/kW), and $v(S)$ is defined as follows [27]:

$$v(S) = \lambda \sum_{k \in S} P_k + \lambda \sum_{i \in S_D, j \in S_P} P_{ij} \quad (20)$$

where P_{ij} represents the power transferred from j to i . The benefit function of MG $_i$ can be defined as:

$$x_i = \lambda \pi_i + \lambda \pi_i^{\text{ex}} \quad (21)$$

where π_i describes the power generated by MG $_i$ in the coalition, and π_i^{ex} represents the total power support from other MGs in the coalition. Assume that every coalition S meets the condition $\sum_{i \in S} N_i = \sum_{i \in S_D, j \in S_P} P_{ij}$, then we know:

$$\begin{cases} x(N) = \lambda \sum_{i \in N} (\pi_i + \pi_i^{\text{ex}}) = \lambda (\sum_{i \in N} P_i + \sum_{m \in S_D, l \in S_P} P_{ml}) \\ = v(N), \quad S'_D \cup S'_P = N \\ x(S) = \lambda \sum_{i \in S} (\pi_i + \pi_i^{\text{ex}}) = \lambda (\sum_{i \in S} P_i + \sum_{i \in S} N_i) \\ = \lambda (\sum_{i \in S} P_i + \sum_{i \in S_D, j \in S_P} P_{ij}) \\ = v(S), \quad S_D \cup S_P = S, \quad \forall S \in N \end{cases} \quad (22)$$

According to condition (19), the allocation strategy of utilizing the remaining dispatchable capacity is optimal. In equation (21), π_i and λ are constants. Hence, an MG with larger π_i^{ex} obtains more benefit. It means that the remaining dispatchable capacity needs to be utilized as much as possible. However, from the dynamic point of view, the MG-wide power generation and demand in a coalition is not always at equilibrium, and λ is a variable. Therefore, it is necessary to design rules to allocate the remaining dispatchable capacity and guide MGs interaction.

When $N_i \neq 0$, MG $_i$ has a decision set $G = \{g_1, g_2\}$, where g_i is the decision variable. Every variable represents the remaining dispatchable capacity in other MGs available to support MG $_i$. Since SBs are more flexible than MTs and can be used for emergency, the remaining dispatchable capacity of SBs should be allocated at the last. Hence g_1 has a higher priority than g_2 . In addition, if g_i comes from more than one MG, it also has a decision set $G_{g_i} = \{g_1^1, \dots, g_n^1\}$. Every decision variable g_n^i represents the capacity of a MG, and the one with more remaining dispatchable capacity has a higher priority. For the convenience of modeling and computing, binary variables are introduced here to mathematically represent priority levels of decision variables. Each decision variable has its own binary variable as a trigger. When trigger conditions are satisfied, the trigger is set to 1, which means the corresponding decision variable is executed. For a decision variable, the trigger conditions are: 1) the previous trigger is 1; if the present trigger has the highest priority level, this condition can be ignored; and 2) MG $_i$ still needs power or power storage support after the previous decision variable is executed. For any MG $_i$ that needs support, the allocation of the remaining dispatchable capacity is made as follows: all decision variables with their triggers are arranged from the highest to the lowest priority levels, and then their triggers are set one by one in the array depending on trigger conditions until all decision variables are allocated. The flow chart of the capacity allocation is shown in Fig. 3.

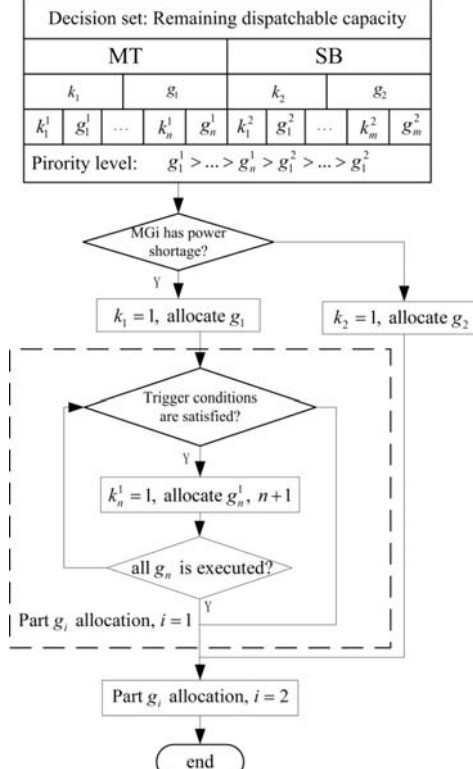


Fig.3.Flow chat of the interactive operation

B. Interactive game matrix

Interactive game matrix (IGM) is a mathematic model to represent and direct the allocation of the remaining dispatchable capacity in the MG cluster. Based on the behavior analysis, the IGM can be described as follows:

$$R_{f,t}^{\text{EX}} = a_{f,t} X_{f,t} P_{f,t}^{\text{MTEX}} + b_{f,t} Y_{f,t} P_{f,t}^{\text{SBEX}} \quad (23)$$

$$X_{f,t} = [x_{h,t} \dots x_{H_i,t}] \quad (24)$$

$$Y_{f,t} = [y_{h,t} \dots y_{H_f,t}] \quad (25)$$

$$P_{f,t}^{\text{MTEX}} = [P_{h,t}^{\text{MTEX}} \dots P_{H_f,t}^{\text{MTEX}}]^T, 0 \leq P_{h,t}^{\text{MTEX}} \leq \alpha_{h,t} \quad (26)$$

$$P_{f,t}^{\text{SBEX}} = [P_{h,t}^{\text{SBEX}} \dots P_{H_f,t}^{\text{SBEX}}]^T, 0 \leq P_{h,t}^{\text{SBEX}} \leq \beta_{h,t} \text{ (power support),} \\ \text{or } \beta_{h,t} - E_{f,t}^{\text{max}} \leq P_{h,t}^{\text{SBEX}} \leq 0 \text{ (power storage support)} \quad (27)$$

$$\alpha_{h,t} = \alpha P_h^{\text{MTmax}} - P_{1,h,t}^G \quad (28)$$

$$\beta_{h,t} = E_{h,t}^T \quad (29) \\ a_{f,t} = \begin{cases} 1 & \text{when } P_{f,t}^{\text{ML}} - \sum_{s \in S_f} P_{s,f,t}^{\text{DG}} > 0 \\ 0 & \text{when } P_{f,t}^{\text{ML}} - \sum_{s \in S_f} P_{s,f,t}^{\text{DG}} \leq 0 \end{cases} \quad (30)$$

$$x_{h,t} = \begin{cases} 1 & \text{when } \alpha_{h,t} = \max \{\alpha_{h',t} \mid h' \in H_f\} \\ & \text{or } \alpha_{h',t} = P_{h',t}^{\text{MTEX}}, \alpha_{h',t} \in \{\alpha_{h'',t} \mid \alpha_{h'',t} > \alpha_{h,t}, h \in H_f\} \\ 0 & \text{other situations} \end{cases} \quad (31)$$

$$b_{f,t} = \begin{cases} 1 & \text{when } P_{f,t}^{\text{ML}} - \sum_{s \in S_f} P_{s,f,t}^{\text{DG}} < 0 \text{ or } \alpha_{h,t} = \\ & P_{h,t}^{\text{MTEX}}, \forall \alpha_{h,t} \in \{\alpha_{h',t} \mid h' \in H_f\} \\ 0 & \text{other situations} \end{cases} \quad (32)$$

$$y_{h,t} = \begin{cases} \text{when } \beta_{h,t} = \max \{\beta_{h',t} \mid h' \in H_f\} \\ \text{or } \beta_{h',t} = P_{h',t}^{\text{SBEX}}, \beta_{h',t} \in \{\beta_{h'',t} \mid \beta_{h'',t} > \beta_{h,t}, h \in H_f\} \\ \text{or } P_{h,t}^{\text{SBEX}} < 0 \\ 0 & \text{other situations} \end{cases} \quad (33)$$

$$C_{f,t} = \frac{\sum_{h \in H_f} [(K_1^{\text{FUEL}} + K_1^{\text{OM}}) P_{h,t}^{\text{MTEX}} + K_2^{\text{OM}} P_{h,t}^{\text{SBEX}}]}{\sum_{h \in H_f} (P_{h,t}^{\text{MTEX}} + P_{h,t}^{\text{SBEX}})} \quad (34)$$

where $i \in I_N$, $h \in H_f$, $P_{f,t}^{\text{MTEX}}$ and $P_{f,t}^{\text{SBEX}}$ are $1 \times H_f$ matrices, $X_{f,t}$ and $Y_{f,t}$ are $H_f \times 1$ matrices. $a_{f,t}$, $b_{f,t}$, $x_{h,t}$, and $y_{h,t}$ are triggers. Trigger conditions are defined in equations (30)-(33). In equation (28), α limits a MT's output within its generation capacity. The flow chart of the IGM is shown in Fig. 4.

In summary, equations (1)-(18) and (23)-(34) represent the proposed interactive model for the coordinated energy management.

V. PROPOSED SOLUTION ALGORITHM

Genetic Algorithm (GA)-based methods have been successfully and widely applied to complex practical optimization problems with enhanced convergence performance [28-29]. In this paper, the authors have improved the traditional Hierarchical Genetic Algorithm (HGA) [30] to make it more suitable for the variable type and relationship of the problem, and solve the proposed mixed-integer program. In HGA, the chromosome coding has two layers: the control gene layer and the parameter gene layer. Control genes are encoded by binaries to control parameter genes. Parameter genes are encoded by real numbers to represent decision variables. When a control gene is set as 1, the corresponding parameter gene is activated. Ordinary genes are also in chromosome coding encoded by real numbers and they are independent of those two types of genes. To better solve the problem, an improved HGA (I-HGA) is presented by adding a superior control gene layer upon the control gene layer to control the control genes. When a superior control gene is set as 1, the

corresponding control gene is activated.

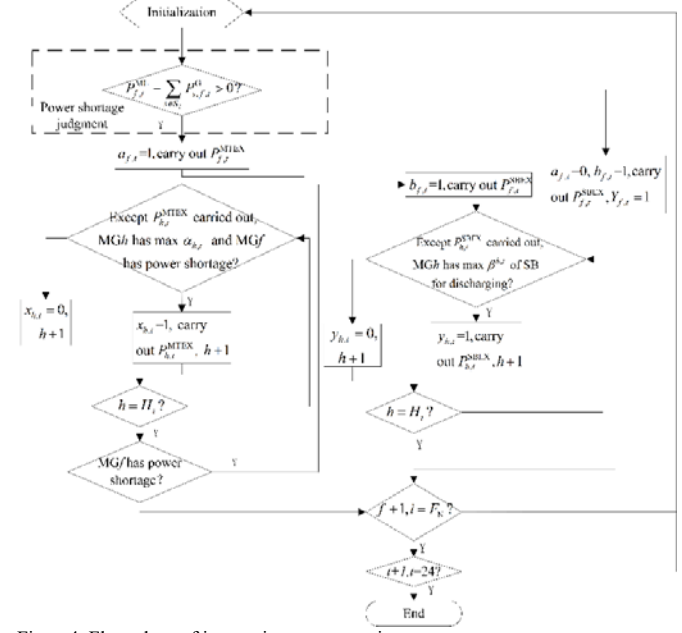


Fig. 4. Flow chart of interactive game matrix

A. Chromosome representation

In the proposed model, the I-HGA chromosome coding is expressed in Fig. 5. Superior control genes are $a_{f,t}$ and $b_{f,t}$. Control genes are $x_{h,t}$ and $y_{h,t}$. $P_{h,t}^{\text{MTEX}}$ and $P_{h,t}^{\text{SBEX}}$ are parameter genes. $Q_{s,f,t}^G$ and $P_{s,f,t}^G$ are ordinary genes.

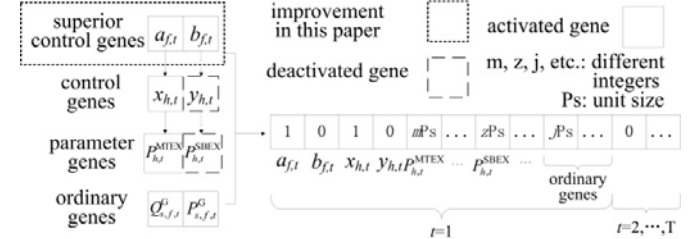


Fig. 5. Chromosome coding of improved hierarchical genetic algorithm

B. Search operators

The chromosomes of the I-HGA are evolved with search operators including crossover and mutation. In this paper, simulated binary crossover (SBX) and non-uniform mutation are applied to the real-coded part of the chromosomes to show better performance compared to other GA variants.

In SBX, child populations $(\psi_i^1 \psi_i^2)$ are generated as follows [31]:

$$\begin{aligned} \psi_i^1 &= 0.5[(1 + \omega_{qi})\phi_i^1 + (1 - \omega_{qi})\phi_i^2] \\ \psi_i^2 &= 0.5[(1 - \omega_{qi})\phi_i^1 + (1 + \omega_{qi})\phi_i^2] \end{aligned} \quad (35)$$

where ω_{qi} is determined as below:

$$\omega_{qi} = \begin{cases} (2u_i)^{1/\eta_c + 1} & u_i \leq 0.5, \\ \left(\frac{1}{2(1-u_i)}\right)^{1/\eta_c + 1} & u_i > 0.5 \end{cases} \quad (36)$$

where u_i is a uniform random number with the range $[0, 1]$ and η_c is a user-defined parameter distribution.

Non-uniform mutation can reduce the step size and has the potential to reduce the number of mutations when the iteration number increases. In the non-uniform mutation, a child is mutated as [29]:

$$\phi_{i,j}^*(g) = \phi_{i,j}(g) + \delta_{i,j}(g) \quad (37)$$

$$\delta_{i,j}(g) = \begin{cases} (\phi_i^{\max} - \phi_{i,j}(g)) \left(1 - [u(g)]^{1-(t/N_G)^b} \right) & u \leq 0.5, \\ (\phi_i^{\max} - \phi_{i,j}(g)) \left(1 - [u(g)]^{1-(g/N_G)^b} \right) & u > 0.5 \end{cases} \quad (38)$$

$$i \in N_{\phi} \text{ and } j \in N_p$$

where $u(g)$ is a random number with the range $[0,1]$. N_p is the number of the population. N_G and g are the maximum generations number and current generation number, respectively.

In each crossover and mutation, the algorithm resets superior control genes and control genes, i.e., the binary-coded part of the chromosomes, according to equations (30)-(33). The main advantage of the I-HGA is that the computational cost is reduced by controlling the evolution of the decision variables with the binary variables.

C. Selection process

The objective function need to be calibrated in order to integrate with the I-HGA. In this paper, a linear calibration method is utilized as shown below [32]:

$$F = f_{\max} - f(x) + \xi^k \quad (39)$$

where $f(x)$ is the objective function, f_{\max} is the maximum value of the objective function in each generation, and k is the k^{th} iteration. ξ^k is a relatively small number. It increases the diversity of the population and promote the convergence in the later evolution stage.

The proportional selection strategy selects child populations according to:

$$\min F = \sum_{i=1}^2 \sigma_i F_i \quad (40)$$

where $\sigma_i = \kappa_i / \sum_{i=1}^2 \kappa_i$, κ_i is a random number with the range $[0,1]$.

D. Steps of the Proposed Algorithm

Steps of the algorithm are described as follows:

Solution feasibility check:

- 1) Substitute every exchange variable (i.e., $P_{i,t}^{\text{PED}}$ and $Q_{i,t}^{\text{PED}}$) of an individual in the upper level into the lower level and calculate the lower model with the I-HGA.
- 2) Check whether there is a solution of the optimization problem in the lower level.

Step 0: Initialization. Set the chromosome, population size and generation=1. Read forecasting data.

Step 1: Create initial population. Check individuals with solution feasibility check. Update individuals not passing the check with new individuals until all individuals in the population pass the judgment.

Step 2: Calculate fitness values according to F^{up} .

Step 3: Let the generation of population do selection.

Step 4: Let the generation of population do crossover and mutation. Check the solution feasibility of the generated individuals. Eliminate individuals that lead to infeasible solutions, and continue crossover and mutation until the next generation of population is formed.

Step 5: If the condition of convergence is satisfied, return the optimal solution and the algorithm ends; otherwise go to step 2.

The above algorithm is established to solve the proposed model.

Fig. 6. depicts the flow chat of the proposed algorithm.

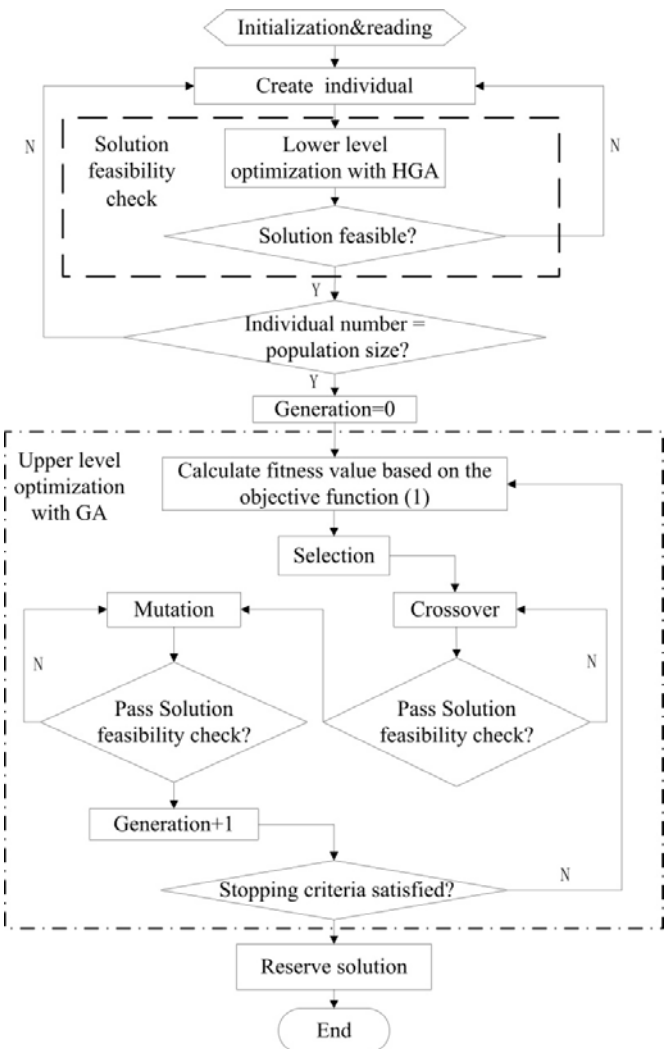


Fig. 6. Flow chat of the proposed algorithm

VI. CASE STUDIES

A. Description of test system

As depicted in Fig. 1, a modified IEEE 14-bus distribution system with three MGs is used in this paper for the purposes of illustration. For this test system, the voltage base is 10.5kV, the total active load is 2870 kW, and the total reactive load is 775 kVAR. 230-kW MTs are connected at nodes 6, 11, and 12. Multiple -100 to 300 kVAR static VAR compensations (SVCs) are connected at nodes 7 and 13. η is set to 8kW. Fig. 7(a) shows the forecasted daily load curves and Fig. 7(b) shows the forecasted daily output curves of PVs and WTs [33]. Table I summarizes the device parameters of MGs. Operating cost parameters and pollution emission penalty of DGs are obtained in [32]. q is set to be 0.61 €/kWh.

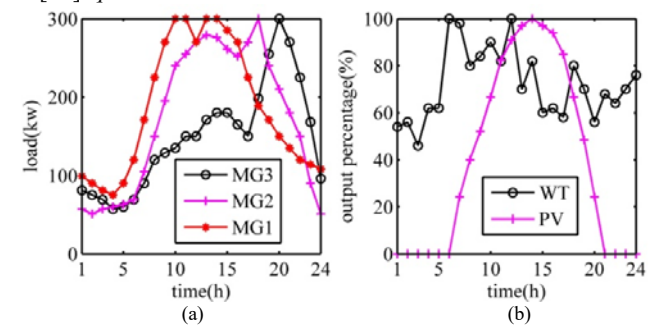


Fig. 7. Forecasted curves: (a) daily load and (b) daily output percentage
Table I. Device parameters of Microgrids

micro-grid	WT max output/ kW	PV max output/ kW	SB max output/ kW	SB capacity/ (kW • h)	MT max output/ kW
MG1	--	210	80	280	185
MG2	250	--	70	320	195
MG3	200	160	80	500	200

To demonstrate the proposed strategy, the following dispatch strategies and cases are considered in this paper.

- Strategy 1: the proposed dispatch strategy
- Strategy 2: the proposed dispatch strategy without the interaction among clustered MGs
- Strategy 3: traditional dispatch strategy whose objective is to minimize total operation costs of the distribution network and MGs
- Case 1: strategy 1 is applied to the distribution system connected with one MG (MG1)
- Case 2: strategy 1 is applied to the distribution system connected with three MGs (MG1, MG2 and MG3)
- Case 3: strategy 2 is applied to the system in case 1
- Case 4: strategy 2 is applied to the system in case 2
- Case 5: strategy 3 is applied to the system in case 1
- Case 6: strategy 3 is applied to the system in case 2
- Case 7: strategy 3 is applied to the distribution system with no MG

The simulations are performed on a PC with a 3.4-GHz Intel Core i7 processor and 16 GB of RAM using the MATLAB (R2015b) environment.

B. Penetration level and power fluctuation of distribution network

The penetration level of intermittent distributed generation (IDG) and the power fluctuation of total power exchange between MGs and distribution network are important indices to evaluate the reliability of a distribution system. Define $s\%$ as the penetration level of IDG, and 0.01s is the proportion of IDG capacity to annual load peak. If the number of MGs including IDGs increases, s increases.

Fig. 8(a) illustrates total power exchanges in cases 5 and 6. As the grid price q is less than the operation cost of a SB, the fluctuation of IDGs and loads in MGs is firstly absorbed by the power exchange with the distribution network. When s increases, the total power exchange increases significantly between -45kW and 240kW.

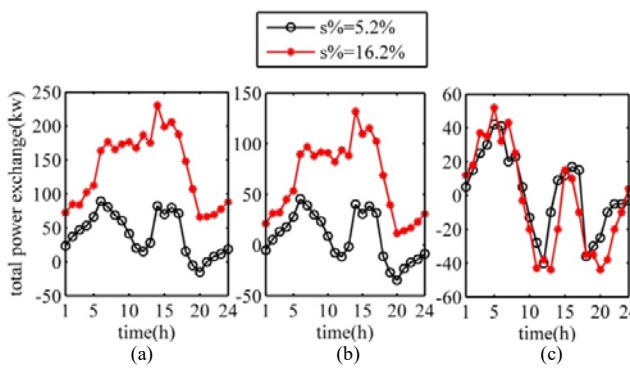


Fig.8. Total power exchanges in different cases: (a) case 5 ($s\% = 5.2\%$) and case 6 ($s\% = 16.2\%$) (b) case 3 ($s\% = 5.2\%$) and case 4 ($s\% = 16.2\%$) (c) case 1 ($s\% = 5.2\%$) and case 2 ($s\% = 16.2\%$)

As depicted in Fig.8(b), the total power exchange is optimized by objective function (3) under the condition of a low penetration level ($s\% = 5.2\%$). When $s = 16.2\%$, since the ability of a single MG to compensate its intermittent power is limited without support from other MGs, the total power exchange becomes higher.

As described in Fig.8(c), due to the cooperative interaction among MGs, the growth of s has smaller impact on the distribution network. The total power exchange is thus within a smaller range between -60kW and 60kW.

In addition, to quantify the effect of smoothing the power fluctuations, the up-down fluctuation value of total power exchange is defined as follows [34]:

$$P_t^{\text{up-down}} = \sum_{i \in I^M} P_{i,t+1}^{\text{PED}} - \sum_{i \in I^M} P_{i,t}^{\text{PED}} \quad (41)$$

As shown in Fig. 9, the power fluctuation is better smoothed in the proposed method compared to the traditional dispatch strategy.

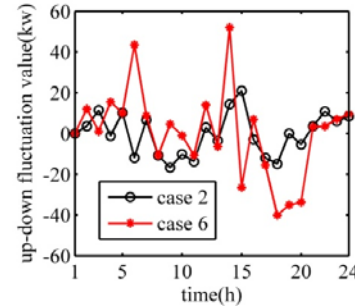


Fig. 9. Comparisons of the effect of smoothing power fluctuation in two cases

C. Peak load shaving

The ability of peak load shaving can help the distribution system reduce power generation costs and relieve generation stress during peak periods. In this paper, every MG is a kind of prosumer [35] to the distribution network. The definition of net load is given as

$$\text{net load} = \text{base (original) load} - \text{MGs output}$$

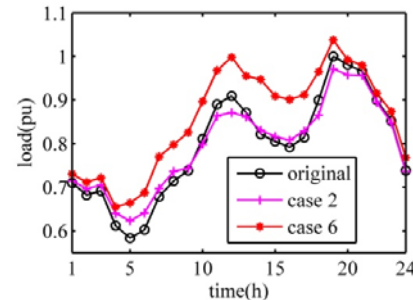


Fig. 10. Load profiles of the distribution network including net load of case 2 and 6

As depicted in Fig. 10, the load difference between peak and valley is 0.3481pu in case 2, which is smaller than 0.3831pu in case 6. Compared to strategy 3, strategy 1 improves the load profile of the distribution network by managing the output of clustered microgrids, i.e., the active power exchange between MG and distribution network.

D. Voltage profile of distribution network

The optimization and regulation of voltages in a distribution network is critical for the system operation. When MGs with a high $s\%$ are integrated, they may cause voltage deviations of the distribution network.

Fig. 11 (a) reveals the difference between the minimum and maximum voltages for representative nodes during the 24-hour dispatching period. It can be seen that voltage deviations in case 2 are smaller than case 6.

As presented in Fig. 11(b), under heavy load condition, voltages are low in case 6, which is more severe at ending nodes. In case 2, voltages at vulnerable nodes are increased effectively by optimizing reactive power.

In Fig. 11(c), voltages of light load are high in case 6. Since the generation of MGs can be more than load consumptions, the reverse power flow results in higher voltages at the terminal of power lines. Case 6 shows that these voltages are kept lower.

Above all, the proposed model improves the voltage profile of the distribution network.

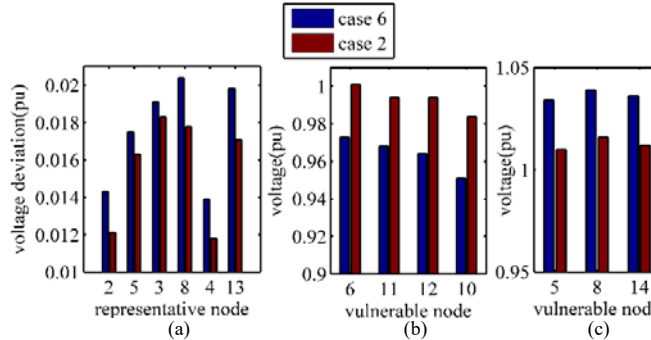


Fig.11.Comparisons of voltage regulation data in two cases: (a) voltage deviations at representative nodes (b) voltage at vulnerable nodes under heavy loading conditions and (c) voltage at vulnerable nodes under light loading condition

E. Power loss of distribution network

As shown in Fig. 12, when there is no MG in the system, the power loss is high. When MGs are connected and the proposed model is applied, the power loss is reduced effectively.

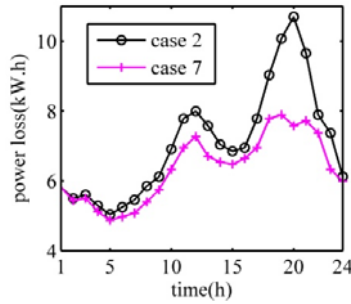


Fig. 12. Comparison of power losses in two cases

F. Responsive reserve support from microgrid cluster

In the proposed model, R_i^{MC} is used for sharing the responsive reserve of the distribution network to enhance the system reliability. We use two indices, the expected demand not supplied (EDNS) [36] and the loss of load probability (LOLP) [37] to evaluate the system reliability. The results in Table II are obtained by utilizing the evaluation method in [36] and [37].

Table II. Distribution System Reliabilities with Different ε

ε	saved responsive reserve of distribution system /kW	LOLP	EDNS/kW
0	0	0.0321	7.25
0.2	24.8	0.0278	4.73
0.4	49.6	0.0271	3.52
0.6	74.4	0.0316	5.94
0.8	99.2	0.0516	10.27
--	--	0.0307	8.97

Table II shows reliability indices and the saved reserve from the distribution system with respect to different ε . Then there is no reserve support ($\varepsilon = 0$) from MGs, the system reliability decreases. The system reliability increases as ε increases within a certain threshold. When ε exceeds the certain threshold (near 0.4), the system reliability decreases. Therefore, the system reliability is improved if an appropriate value of ε is selected.

G. Environmental costs

The 24-hour environmental cost f_2 is €6370 in case 2, and €10690 in case 6. By applying the proposed method, the environmental cost has been reduced by 40.4%. On the other hand, SB utilization ratio during the entire operation period is 92.6% in case 2, which is higher than 71.3% in case 6. It means that the decrease of environmental cost represents the decrease of MT output which produces pollution. Due to IGM, if there is surplus IDG output which cannot be stored by the local MG at a certain period, this power can be stored by the SB of other MGs rather than consumed by the distribution network. When there is a power shortage, this stored power can compensate the shortage. Therefore, the renewable energy utilization can be improved.

H. Performance of the proposed algorithm

The proposed I-HAG has been implemented in a practical microgrid project in China. The project is based on a real energy system (renewable energy resource (RER)-based distribution system) with 7 energy hubs (MGs) in Shandong Province, China. Due to data confidentiality, we only provide the details that are important to understand results. The single line diagram of the real system and essential equipment are shown in Fig. 13. Table III shows capacities of DGs and storage batters in the system.

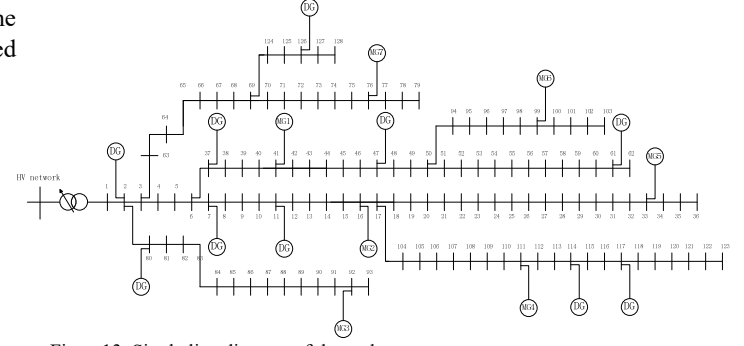


Fig. 13. Single line diagram of the real system
 Table III. Capacities of DGs and storage batteries in each microgrid

micro-grid	WT total maximum output/kW	PV total maximum output/kW	SB total maximum output/kW	SB total capacity/(kW·h)	MT total maximum output/kW
MG1-2	800	750	500	1500	800
MG3-4	750	500	500	1500	1050
MG5-7	1000	1200	1000	2500	1800

Local renewable energy generators and load outputs are received from the historical data of the project. η is set to be 20kW. The remaining data and parameters are derived from the project and previous case studies in the paper. This system is denoted as ‘test system 2’ and the IEEE 14-bus distribution system with three MGs in Fig. 1 is denoted as ‘test system 1’.

To illustrate the effectiveness of I-HGA, 50 independent simulation runs are performed for each test system with the proposed model in this paper and the solutions are recorded and compared with the results from the-state-of-the-art algorithms [38] including improved genetic algorithm (IGA) [39], improved particle swarm optimization (IPSO) [40], modified teaching-learning algorithm (MTLA) [41], chaotic sequence-based differential evolution (CSDE) [42] and evolutionary programming-sequential quadratic programming (EP-SQP) [43]. The same simulation platform is utilized. Table IV and V show the comparison results.

Table IV. Comparison among different methods in test system 1

Method	Optimal solution F^{up}			Average number of	Average CPU time (s)
	Minimum	Average	Maximum		

	(Best)	(Worst)	iterations	
I-HGA	243.28	244.76	245.52	210
IGA	244.09	245.38	247.66	224
IPSO	247.18	248.26	251.63	383
MTLA	244.84	246.39	247.80	267
CSDE	245.52	247.33	249.26	319
EP-SQP	251.47	253.48	256.12	467
Table V. Comparison among different methods in test system 2				

Table V. Comparison among different methods in test system 2

Method	Optimal solution F^{opt}			Average number of iterations	Average CPU time (s)
	Minimum (Best)	Average	Maximum (Worst)		
I-HGA	471.60	473.21	475.60	639	78.10
IGA	472.67	473.64	476.10	682	102.02
IPSO	475.35	476.57	479.95	1159	123.41
MTLA	473.34	474.57	476.07	801	92.42
CSDE	474.09	475.41	477.83	957	135.75
EP-SQP	479.58	481.82	484.66	1410	162.42

It can be seen that compared with other commonly used optimization algorithms [44], I-HGA can achieve better solutions with the least average number of iterations and the best average computational performance.

Besides, the deviations of the best and worst solutions of the proposed I-HGA from the corresponding average result for each test system are calculated as follows [45]:

$$\text{Deviation of the Best Solution from the Average} \\ \text{Result}(\%) = \frac{|\text{Best Solution} - \text{Average Result}|}{\text{Average Result}} \quad (42)$$

$$\text{Deviation of the Worst Solution from the Average} \\ \text{Result}(\%) = \frac{|\text{Worst Solution} - \text{Average Result}|}{\text{Average Result}} \quad (43)$$

Table VI. Deviation of the best and worst solutions of the proposed I-HGA from the corresponding average result in terms of percentage

Test system	Deviation of the Best Solution from the Average	Deviation of the Worst Solution from the Average
	Result(%)	Result(%)
1	0.34	0.51
2	0.60	0.31

The results of Table VI show that the best, average, and worst solutions of the proposed I-HGA are close to each other, which indicates stability of the results of the I-HGA [45].

VII. CONCLUSIONS

In this paper, an interactive model for coordinated energy management of a distribution system with clustered MGs is proposed. There are two levels in the proposed optimization model. The upper level is to reduce power loss, improve voltage profile, and smooth power fluctuation for distribution network operation. The lower level is to reduce operation costs and pollution emission for MGs operation. A power reserve mechanism and a game theory-based strategy are introduced to coordinate the interaction between MGs and the distribution network. A modified HGA is used for solving the proposed hierarchical model. Simulations on a modified IEEE 14-buse distribution system with 3 MGs and a practical multi-MG test system demonstrate the effectiveness of the proposed approach. The proposed method considers benefits and operation performances of each entity. Furthermore, it has reduced power losses by 12.7%, average power fluctuations by 56.8%, average voltage deviations by 9.1%, and environmental costs by 40.4%. Last but not least, with a proper allocation of responsive reserve from MGs to support the distribution system, the system reliability has increased.

VIII. ACKNOWLEDGEMENT

This work is partially supported by National Natural Science Foundation of China (No. 51577115), and Iowa Energy Center.

REFERENCES

- [1] Z. Wang, and J. Wang, "Self-healing resilient distribution systems based on sectionalization into microgrids," *IEEE Trans. Smart Grid*, vol. 30, no. 6, pp. 3139-3149, Nov. 2015.
- [2] Z. Wang, B. Chen, J. Wang, J. Kim, and M. M. Begovic, "Robust optimization based optimal dg placement in microgrids," *IEEE Trans. Smart Grid*, vol. 5, no. 5, pp. 2173-2182, Sep. 2014.
- [3] C. D. Adamo, S. Jupe, C. Abbey, "Global survey on planning and operation of active distribution networks-update of cigre c6.11 working group activities," in *20th International Conference on Electricity Distribution*, Prague, Jun. 2009.
- [4] A. Iapkchi and F. Albuyeh, "Grid of the future," *IEEE Power Energy Mag.*, vol. 7, no. 2, pp. 52-62, Mar.-Apr. 2009.
- [5] G. Venkataraman and C. Marnay, "A larger role for microgrids," *IEEE Power and Energy Mag.*, vol. 6, no. 3, May 2008.
- [6] N. Jayawarna, C. Jones, M. Barnes, and N. Jenkins, "Operating microgrid energy storage control during network faults," in *IEEE International Conference on Systems Engineering*, San Antonio, Texas, Apr. 2007.
- [7] S. Ahn, J. Park, I. Chung, S. Moon, S. Kang, and S. Nam, "Powersharing method of multiple distributed generators considering control modes and configurations of a microgrid," *IEEE Trans. Power Del.*, vol. 25, no. 3, Jul. 2010.
- [8] N. Soni, S. Doolla, and M. C. Chandorkar, "Improvement of transient response in microgrids using virtual inertia," *IEEE Trans. Power Del.*, vol. 28, no. 3, pp. 1830-1838, Jul. 2013.
- [9] R. H. Lasseter, "Smart distribution: Coupled microgrids," *Proc. IEEE*, vol. 99, pp. 1074-1082, Jun. 2011.
- [10] Q.-C. Zhong, "Robust droop controller for accurate proportional loadsharing among inverters operated in parallel," *IEEE Trans. Ind. Electron.*, vol. 60, no. 4, pp. 1281-1290, 2013.
- [11] O. Samuelsson, S. Repo, R. Jessler, J. Aho, M. Karenlampi, and A. Malmquist, "Active distribution network—Demonstration project ADINE," in *Proc. IEEE PES Innovative Smart Grid Technologies Conf. Europe (ISGT Europe)*, Oct. 2010.
- [12] Y. Levron, J. M. Guerrero, and Y. Beck, "Optimal power flow in microgrids with energy storage," *IEEE Trans. Power Syst.*, vol. 28, no. 3, pp. 3226-3234, Aug. 2013.
- [13] J. C. Vasquez, J. M. Guerrero, J. Miret, and M. Castilla, "Hierarchical control of intelligent microgrids," *IEEE Ind. Electron. Mag.*, vol. 4, no. 4, pp. 23-29, Dec. 2010.
- [14] B. Zhao, M. Xue, X. Zhang, C. Wang, and J. Zhao, "An MAS based energy management system for a stand-alone microgrid at high altitude," *Appl. Energy*, vol. 143, pp. 251-261, Apr. 2015.
- [15] J. Wasilewski, "Integrated modeling of microgrid for steady-state analysis using modified concept of multi-carrier energy hub," *Int. J. Electr. Power Energy Syst.*, vol. 73, pp. 891-898, Dec. 2015.
- [16] G. E. Asimakopoulou, A. L. Dimeas, and N. D. Hatziargyriou, "Leader-follower strategies for energy management of multi-microgrids," *IEEE Trans. Smart Grid*, vol. 4, no. 4, pp. 1909-1916, Dec. 2013.
- [17] N. Nikmehr and S. N. Ravanagh, "Optimal power dispatch of multi-microgrids at future smart distribution grids," *IEEE Trans. Smart Grid*, accepted online.
- [18] C. D. Korkas, S. Baldi, I. Michailidis, and E. B. Kosmatopoulos, "Intelligent energy and thermal comfort management in grid-connected microgrids with heterogeneous occupancy schedule," *Appl. Energy*, vol. 149, pp. 194-203, Jul. 2015.
- [19] H. S. V. S. Kumar Nunna and S. Doolla, "Demand response in smart distribution system with multiple microgrids," *IEEE Trans. Smart Grid*, vol. 3, no. 4, pp. 1641-1649, Dec. 2012.
- [20] M. Fathi and H. Bevrani, "Statistical cooperative power dispatching in interconnected microgrids," *IEEE Trans. Sustain. Energy*, vol. 4, no. 3, pp. 586-593, Jul. 2013.
- [21] Z. Wang, B. Chen, J. Wang, and M. M. Begovic, "Coordinated energy management of networked microgrids in distribution systems," *IEEE Trans. Smart Grid*, vol. 6, no. 1, pp. 45-53, Jan. 2015.

- [22] T. Lv, Z. Wang, Q. Ai and W. Lee, "Interactive model for energy management of clustered microgrids," in *2016 IEEE Industry Applications Society Annual Meeting*, Portland, Oregon, Oct. 2016.
- [23] T. Lv, Q. Ai, and Y. Zhao, "A bi-level multi-objective optimal operation of grid-connected microgrids," *Electr. Power Syst. Res.*, vol. 131, pp. 60-70, Feb. 2016.
- [24] T. Lv, and Q. Ai, "Interactive energy management of networked microgrids-based active distribution system considering large-scale integration of renewable energy resources," *Appl. Energy*, vol. 163, pp. 408-4222, Feb. 2016.
- [25] J. Lin, Y. Sun, L. Cheng, and W. Gao, "Assessment of the power reduction of wind farms under extreme wind condition by a high resolution simulation model," *Appl. Energy*, vol. 96, pp. 21-32, Aug. 2012.
- [26] C. Wei, Z. M. Fadlullah, N. Kato, and A. Takeuchi, "GT-CFS: A gametheoretic coalition formulation strategy for reducing power loss in microgrids," *IEEE Trans. Parallel Distrib. Syst.*, vol. 25, no. 9, pp. 2307-2317, Sep. 2014.
- [27] L. Kwang-Ho, and R. Baldick, "Solving three-player games by the matrix approach with application to an electric power market," *IEEE Trans. Power Syst.*, vol. 18, no. 4, pp. 1573-1580, Mar. 2003.
- [28] J. Liu, and J. Li, "A bi-level energy-saving dispatch in smart grid considering interaction between generation and load" *IEEE Trans. Smart Grid*, vol. 6, no. 3, pp. 1443-1452, May 2015.
- [29] M. F. Zaman, S. M. Elsayed, T. Ray, and R. A. Sarker, "Evolutionary algorithms for dynamic economic dispatch problems" *IEEE Trans. Power Syst.*, vol. 31, no. 2, pp. 1486-1495, Mar. 2016.
- [30] R. Kumar, K. Izui, Y. Masataka, and S. Nishiwaki, " Multilevel RedundancyAllocation Optimization Using Hierarchical Genetic Algorithm," *IEEE Trans. Reliab.*, vol. 57, no. 4, pp. 650-661, Mar. 2008.
- [31] K. Deb, A. Pratap, S. Agarwal, and T. Meyarivan, "A fast and elitist multiobjective genetic algorithm: NSGA-II," *IEEE Trans. Evol. Computat.*, vol. 6, no. 2, pp. 182 - 197, 2002.
- [32] Y. Zhao, Y. An, and Q. Ai, "Research on size and location of distributed generation with vulnerable node identification in the active distribution network," *IET Gener. Transm. & Distrib.*, vol. 8, pp. 1801-1809, Mar. 2014.
- [33] J. Chen, X. Yang, L. Zhu, M. Zhang, and Z. Li, "Microgrid multi-objective economic dispatch optimization," *Proceedings of the CSEE*, vol.33, no.19, pp. 57-66, Jul. 2013.
- [34] Y. Attwa, E. F. El-Saadany, M. M. A. Salama, and R. Seethapathy, "Optimal renewable resources mix for distribution system energy loss minimization," *IEEE Trans. Power Syst.*, vol. 25, no. 1, pp. 360-370, Feb. 2010.
- [35] N. Zhang, Y. Yan, and W. Su, "A game-theoretic economic operation of residential distribution system with high participation of distributed electricity prosumers" *Appl. Energy*, pp. 154:471-9, 2015.
- [36] R. A. Bakkiyraj, and N. Kumarappan, "Reliability design of composite generation and transmission system based on Latin Hypercube Sampling with GRNN state adequacy evaluation." in *Sustainable Energy and Intelligent Systems (SEISCON 2013)*, IET Chennai Fourth International Conference on, Dec. 2013.
- [37] S. S. Singh, and E. Fernandez, "Method for evaluating battery size based on loss of load probability concept for a remote PV system." in *6th IEEE Power India International Conference (PIICON)*, Delhi, India, Dec. 2014.
- [38] C. Shang, D. Srinivasan and T. Reindl, "Economic and environmental generation and voyage scheduling of all-electric ships" *IEEE Trans. Power Syst.*, vol. 31, no. 5, pp. 4087-4096, Sep. 2016.
- [39] S. H. Ling and F. H. F. Leung, "An Improved genetic algorithm with average-bound crossover and wavelet mutation operations," *Soft Comput.*, vol. 11, no. 1, pp. 7-31, Jan. 2007.
- [40] B. Mohammadi-Ivatloo, A. Rabiee, and M. Ehsan, " Time-varying acceleration coefficients IPSO for solving dynamic economic dispatch with non-smooth cost function," *Energy Convers. Manage.*, vol. 56, no. 0, pp. 175 - 183, 2012.
- [41] T. Niknam, R. Azizipanah-Abarghooee, and J. Aghaei, "A new modified teaching-learning algorithm for reserve constrained dynamic economic dispatch," *IEEE Trans. Power Syst.*, vol. 28, no. 2, pp. 749-763, May 2013.
- [42] D. He, G. Dong, F. Wang, and Z. Mao, "Optimization of dynamic economic dispatch with valve-point effect using chaotic sequence based differential evolution algorithms," *Energy Convers. Manage.*, vol. 52, no. 2, pp. 1026-1032, 2011.
- [43] P. Attaviriyapanupap, H. Kita, E. Tanaka, and J. Hasegawa, "A hybrid EP and SQP for dynamic economic dispatch with nonsmooth fuel cost function," *IEEE Trans. Power Syst.*, vol. 22, no. 4, p. 77, Nov. 2002.
- [44] S. Ma, B. Chen, and Z. Wang, "Resilience enhancement strategy for distribution systems under extreme weather events," *IEEE Trans. Smart Grid*, to be published.
- [45] N. Amjadi, and H. Nasiri-Rad, "Nonconvex economic dispatch with ac constraints by a new real coded genetic algorithm" *IEEE Trans. Power Syst.*, vol. 24, no. 3, pp. 1489-1502, Aug. 2009.



Tianguang Lu (S'16) received the B.S. degree in electrical engineering from Shandong University, Shandong, China, in 2013. He is currently working toward the Ph.D. degree at the School of Electronic Information and Electrical Engineering, Shanghai Jiaotong University, Shanghai, China.

He was an Electrical Engineer Intern with ABB (China) Inc. in 2015, and a Visiting Student Researcher with The University of Texas at Arlington, Arlington, TX, USA, in 2016. He is currently a Visiting Student Researcher with Iowa State University, Ames, IA, USA. His research interests include power distribution systems, microgrids, and renewable energy. His research is supported by National Natural Science Foundation of China.



Zhaoyu Wang (M'15) is an Assistant Professor with Iowa State University. He received the B.S. and M.S. degrees in electrical engineering from Shanghai Jiaotong University in 2009 and 2012, respectively, and the M.S. and Ph.D. degrees in electrical and computer engineering from Georgia Institute of Technology in 2012 and 2015, respectively.

He was a Research Aid at Argonne National Laboratory in 2013, and an Electrical Engineer at Corning Inc. in 2014. His research interests include power distribution systems, microgrids, renewable integration, power system resiliency, demand response and voltage/VAR control.

Dr. Wang is an editor of IEEE TRANSACTIONS ON SMART GRID and IEEE POWER ENGINEERING LETTERS. His research projects are currently funded by National Science Foundation, the Department of Energy, National Laboratories, PSERC, Iowa Energy Center and industry.



Qian Ai (M'03, SM'16) received the Bachelor's degree from Shanghai Jiao Tong University, Shanghai, China; the Master's degree from Wuhan University, Wuhan, China; and the Ph.D. degree from Tsinghua University, Beijing, China, in 1991, 1994, and 1999, respectively, all in electrical engineering.

He was with Nanyang Technological University, Singapore, for one year; the University of Bath, Bath, U.K., for two years; and then with Shanghai Jiao Tong University, where he is currently a Professor with the School of Electronic Information and Electrical Engineering. His current research interests include power quality, load modeling, smart grids, microgrid, and intelligent algorithms.



Wei-Jen Lee (S'85-M'85-SM'97-F'07) received the B.S. and M.S. degrees from National Taiwan University, Taipei, Taiwan, R.O.C., and the Ph.D. degree from the University of Texas, Arlington, in 1978, 1980, and 1985, respectively, all in Electrical Engineering.

He is currently a professor of the Electrical Engineering Department and the director of the Energy Systems Research Center. Prof. Lee has been involved in research on arc flash and electrical safety, utility deregulation, renewable energy, smart grid, microgrid, load forecasting, power quality, distribution automation and demand side management, power systems analysis, online real time equipment diagnostic and prognostic system, and microcomputer based instrumentation for power systems monitoring, measurement, control, and protection. Since 2008 he has also served as the project manager for the IEEE/NFPA Arc Flash Research Project.

Prof. Lee is a Fellow of IEEE and registered Professional Engineer in the State of Texas.